BOULDER DENSITIES AT THE COMPTON-BELKOVICH VOLCANIC COMPLEX.

N. J. Accardo[1], B. L. Jolliff[1], and S. J. Lawrence, [1]Dept. Earth & Planetary Sciences and The McDonnell Center for the Space Sciences, Washington University, One Brookings Drive, St. Louis, MO 63130, [2]School of Earth and Space Exploration, Arizona State University, Tempe, AZ. (natalie.accardo@wustl.edu)

Introduction: Photographs from the Ranger mission in 1965 [1] first revealed the presence of boulders on the lunar surface. In the decades since, images have shown boulders to occur most commonly in close proximity to large impact craters pointing to an impact-induced origin. Recently, high resolution images (0.5 m/pixel) from the Lunar Reconnaissance Orbiter (LRO) Narrow Angle Camera (NAC) have revealed substantial boulder populations occurring on other geologic landforms such as domes, lava flows, and mare wrinkle ridges [2-3]. These populations are not proximal to large impact craters, suggesting a non-impact origin. In this study we focus on the Compton-Belkovich Volcanic Complex (CBVC), a small, silicic volcanic terrain located at ~99.8° E Lon, 61.3° N Lat. [3]. This region is characterized by a thorium-rich orbital compositional anomaly (Lunar Prospector gamma-ray data), relatively reflective terrain, locally elevated topography (LRO LOLA, WAC, and NAC), and silicic composition (LRO Diviner) [4]. We directly measure boulder size distributions associated with 3 topographically distinct mounds within the CBVC that range from a dome with slopes approaching 30 degrees (mound 1) to a low mound or "bulge" (mound 7) (Fig. 1). These results contribute to the characterization of boulders formed by processes other than impact, which should enable a greater understanding of physical properties of the rock types that make up the boulders, to distinguishing the style of eruption, and to understanding the properties of Compton-Belkovich volcanic materials.

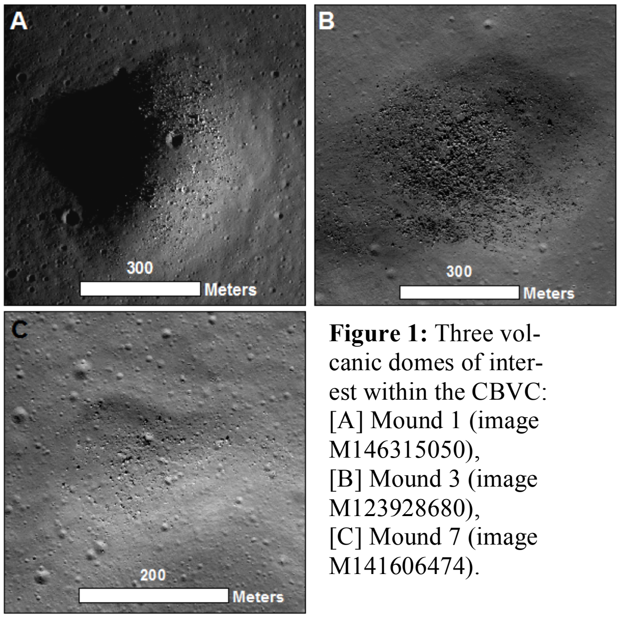

Figure 1: Three volcanic domes of interest within the CBVC: [A] Mound 1 (image M146315050), [B] Mound 3 (image M123928680), [C] Mound 7 (image M141606474).

Methods: We follow the methods of [5-6] and define a "boulder" as an apparently intact rock or rock fragment. In images we identify boulders as positive relief features that correspond to bright pixels on the sunward side of dark pixels (which readily distinguishes them from small craters). For the work reported here, we analyzed boulder fields associated with 3 distinct small domes within the CBVC using high-resolution (~ 0.5 mpp) images from the LRO NAC.

To perform these analysis, we identified the locations of boulders and measured their diameter. We analyzed the images with the computer program ArcMap (ESRI's ArcGIS) and specifically the extension CraterTools [7]. CraterTools was chosen primarily because it is a toolbox intended for measuring crater size frequency distributions, but can be applied to boulder distributions. For each boulder, the center of the diameter measurement was taken as its location. All measurements of diameter were made on the longest observable axis, which most often corresponds to that perpendicular to the Sun's direction. In part this results from the fact that the CBVC is located at ~61 N latitude, so prominent shadows are associated with boulders under all illumination conditions.

We acknowledge three main sources of error with our methods: 1) viewing geometry, 2) image resolution, and 3) overlying or closely clustered boulders. To best differentiate boulders from the surrounding surface, high incidence angles are ideal (e.g., > 60°). However, these high angles of incidence lead to long shadows, which can partially or entirely hide boulders within shadowed regions and in the shadows of other boulders. While the LRO NAC allows for better resolution than ever before, we have adopted a conservative approach, and do not consider detections of boulders less than 4 pixels in area (i.e., 1 m in diameter) to be reliable. Furthermore, resolution limitations likely lead to a mismatch between the measured boulder diameter and the actual boulder diameter. We therefore assume an uncertainty of ± 0.5 m (i.e., 1 pixel). Finally, in these occurrences, boulders commonly overlie other boulders, which obstructs our view of the underlying boulders. Because of the limitations of viewing geometry, image resolution, and overlying boulders, we assume that our counts somewhat under-represent the true population of boulders on these mounds [8].

Results: Combined we counted over 7,000 boulders between 1 and 14 m in diameter at the three different locations. The individual statistics for each mound can be seen in Table 1. Boulder density was calculated as the percentage of mound area covered by boulders (boulder area was calculated assuming the boulders in plan view are perfect circles). Although the exact distributions vary, we found a mean diameter of 3.28 m with a mode of 2.38 m; 68% of the boulder diameters were between 1.73 and 4.84 m. Histograms of all three boulder populations are skewed to the right, toward larger diameters [Fig. 2].

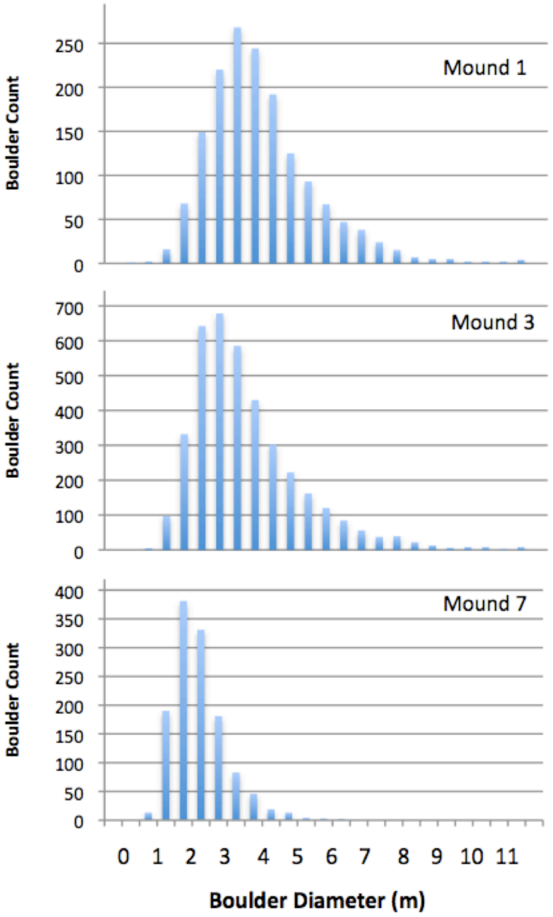

Figure 2. Histograms of boulder diameters in meters for the three domes of interest.

Discussion: The boulder populations for the three domes investigated vary significantly but systematically. The largest boulders occur on Mound 1 (mean diam. = 3.92 m) which was also the dome with the least amount of surface area covered by boulders and the one with steepest slopes. The smallest boulders occur on Mound 7 (mean diam. = 2.21 m) and on average are more than a meter smaller than those found on either Mound 1 or Mound 3. Mound 7 is the smallest and most topographically subdued of the three mounds investigated. Mound 3 which is the largest of the three domes investigated. Mound 3 has the most boulders and the largest amount of surface area covered by boulders (approximately 22%).

Future Work: Larger volcanic constructs also occur at the CBVC, for example, the elongate β dome [9] has associated boulder fields, but these occur in patches. Other, larger volcanic constructs do not have such associated boulder fields. We are determining these boulders distributions where they occur to further our understanding of the underlying volcanic materials.

Acknowledgements: We gratefully acknowledge NASA's support of the LRO mission and the hard work of the LROC Operations Team in collecting the images used for this research.

References: [1] Kuiper G. P. et al. (1965) *The Nature of the Lunar Surface,* 99-105. [2] Robinson M. A. et al. (2010) *Space Science Reviews* **150**, 81-124. [3] Lawrence S. J. et al. (2011) *Lunar Planet Sci.* **42**, Abstract #2422. [4] Jolliff B. L. et al., (2011) *Nature Geoscience* **4**, 566-571 [5] Bart G. et al, (2010) *Icarus* **209**, 337-357. [6] Bart G. et al, (2007) *Geophysical Research Letters* **34,** 1-5. [7] Kneissl T. et al. (2011) *Planetary and Space Science* **59**, 1243-1254. [8] Bandfield J. L. et al (2011) *Journal of Geophysical Research* **116**. [9] Jolliff B. L. et al. (2012) *Lunar Planet Sci.* **43**, this Conf.

Table 1: Statistical parameters from boulder frequency distributions at Mounds 1, 3, 7, and combined. Statistics were calculated from the statistical package StatPlus: Mac 2009^{TM}.

Parameter	Mound 1	Mound 3	Mound 7	Total
Boulder Count	1596	4690	1266	7139
Mean Boulder Size (m)	3.916	3.513	2.207	3.283
Mode	3.968	2.381	1.87	2.38
Skewness	1.23	1.66	1.32	1.56
Area of Dome (km^2)	0.215	0.253	0.0334	0.502
Boulder Density	10.75 %	21.99 %	16.90 %	16.81%
Boulder Frequency (count per km^2)	7423	18,538	37,904	14,221